



Life and death of *Pseudokirchneriella subcapitata*: physiological changes during chronological aging

Manuela D. Machado^{1,2,3} · Eduardo V. Soares^{1,2,3}

Received: 6 September 2022 / Revised: 20 October 2022 / Accepted: 23 October 2022 / Published online: 17 November 2022
© The Author(s), under exclusive licence to Springer-Verlag GmbH Germany, part of Springer Nature 2022

Abstract

The green alga *Pseudokirchneriella subcapitata* is widely used in ecotoxicity assays and has great biotechnological potential as feedstock. This work aims to characterize the physiology of this alga associated with the aging resulting from the incubation of cells for 21 days, in the OECD medium, with continuous agitation and light exposure, in a batch mode. After inoculation, cells grow exponentially during 3 days, and the culture presents a typical green color. In this phase, “young” algal cells present, predominantly, a lunate morphology with the chloroplast occupying a large part of the cell, maximum photosynthetic activity and pigments concentration, and produce starch as a reserve material. Between the 5th and the 12th days of incubation, cells are in the stationary phase. The culture becomes less green, and the cells stop dividing ($\geq 99\%$ have one nucleus) and start to age. “Old” algal cells present chloroplast shrinkage, an abrupt decline of chlorophylls content, and photosynthetic capacity (F_v/F_m and Φ_{PSII}), accompanied by a degradation of starch and an increase of neutral lipids content. The onset of the death phase occurs after the 12th day and is characterized by the loss of cell membrane integrity of some algae (cell death). The culture stays, progressively, yellow, and the majority of the population ($\sim 93\%$) is composed of live cells, chronologically “old,” with a significant drop in photosynthetic activity (decay $> 75\%$ of F_v/F_m and Φ_{PSII}) and starch content. The information here achieved can be helpful when exploring the potential of this alga in toxicity studies or in biotechnological applications.

Key points

- *Physiological changes of P. subcapitata with chronological aging are shown*
- *“Young” algae exhibit a semilunar shape, high photosynthetic activity, and accumulated starch*
- *“Old”-live algae show reduced photosynthetic capacity and accumulated lipids*

Keywords Cell-division cycle · Cell death · Conditional senescence · Photosynthesis · Stationary phase · Reserve material (starch and lipids)

Introduction

Microalgae have attracted growing interest mainly due to their biological, ecological, and economical potential. Moreover, as primary producers, microalgae sustain life in oceans being a fundamental ecological player in the maintenance of the flow of energy and nutrients through ecosystems (Naselli-Flores and Padišák 2022). From an economic point of view, microalgae and their by-products are used as food resources, in pharmaceutical industry and in health supplements, cosmetics, biofuels, and agriculture (Borowitzka 2013; Khan et al. 2018; Koller et al. 2014). Microalgae are also applied in toxicity assessment due to their ease of culturing, low nutritional requirements, fast cellular division, and sensitivity to pollutants (Cid et al. 2013). *Pseudokirchneriella subcapitata*

✉ Manuela D. Machado
mmmachado@net.sapo.pt

✉ Eduardo V. Soares
evs@isep.ipp.pt

¹ Bioengineering Laboratory, ISEP-School of Engineering, Polytechnic Institute of Porto, Rua Dr António Bernardino de Almeida, 431, 4249-015 Porto, Portugal

² CEB - Centre of Biological Engineering, University of Minho, Campus de Gualtar, 4710-057 Braga, Portugal

³ LABBELS – Associate Laboratory, Braga/Guimarães, Portugal

is one of the most frequently used species of microalgae in freshwater toxicity tests, with a vast database of responses to a wide diversity of pollutants, being recommended by regulatory agencies (OECD 2011; US-EPA 2002). However, these data need to be analyzed carefully as *P. subcapitata* cells that are often incubated for different time intervals do not show the same physiological conditions.

One of the most common constraints on microalgae growth is the use of extended times of cultivation which can lead to nutrient deprivation. Nutritional privation is also common in nature. It is known that reduced availability of nutrients can affect growth rate and cellular composition. For instance, it is described that the bioavailability of phosphorus and nitrogen influences the content and composition of lipids in microalgae (Bondioli et al. 2012; Gao et al. 2013). Moreover, bioproduct formation may not occur in parallel with biomass growth (Atikij et al. 2019; Teh et al. 2021). Thus, the development of high-productivity systems to obtain high-value by-products implies the knowledge of the physiological status of microalgae along the culture time. Morphological, biochemical, and functional changes that occurred during the culture of algae can be good bioindicators of the health status of the population, which can be crucial for the maximization of the yield of the production of foods and high-value bioproducts.

Microalgae can be considered “immortal” as, theoretically, they can divide indefinitely if have nutrients and the appropriate conditions. However, the permanence of microalgae in culture medium, in batch mode, after the exponential phase of growth, results in nutrient deprivation and led to the aging of the cells (chronological aging, also known as conditional senescence), i.e., the cell deterioration over time (Florea 2017). This aging process is well-studied in bacteria (Nyström 2003), ciliate protozoa (Petralia et al. 2014), and, particularly, yeasts (Gershon and Gershon 2000; Longo et al. 2012). Nevertheless, limited information is available about the aging of microalgae. Studies with *Chlamydomonas reinhardtii* and *Spongiocloris typica* showed that when algae enter into a stationary phase of growth, as a result of nutrient deprivation, in an attempt to prolong their longevity, they produce reserve compounds, thicken their walls, and may change their color and change their metabolome (Damoo and Durnford 2021; McLean 1969; Puzanskiy et al. 2018). However, as far as we know, there is no information about the mechanisms of chronological aging in *P. subcapitata*, an important cell model in toxicology and biotechnology.

The present work aims to reveal the physiological alterations of the alga *P. subcapitata* during the prolonged culture in the OECD medium, in a batch mode. For that purpose, the number of cells, the loss of cell membrane integrity, the cell shape, the cell-division cycle progression, the lipid and carbohydrates content, the pigments, and the photosynthetic performance were assessed during the incubation period of

21 days. The usefulness of the observed structural, biochemical, and functional modifications of *P. subcapitata* cells as feature markers of the “health” status of the alga (and of the culture) will be discussed.

Material and methods

Strain and culture conditions

The freshwater microalga *P. subcapitata*, strain 278/4, was obtained from the Culture Collection of Algae and Protozoa (CCAP, UK). Cultures were performed by inoculating algal cells, in exponential phase of growth (2 days), at an initial concentration of 1×10^5 cells mL⁻¹, in 400 mL of OECD medium (OECD 2011), and in a 1-L Erlenmeyer flask. Cells were incubated at 25 °C, on an orbital shaker, at 100 rpm, under uninterrupted light, obtained through the use of fluorescent lamps, placed on the top of the cultures, with a color temperature of 4300 K and an intensity of 4000 lux ($\sim 54 \mu\text{mol photons m}^{-2} \text{s}^{-1}$), and measured at the base of the Erlenmeyer flask using an illumination meter.

At the times indicated in the figures, samples were taken to study the physiology of the algae. Cell concentration was measured using an automatic cell counter (TC10, Bio-Rad Laboratories, Inc, Hercules, CA, USA). The generation time (doubling time) of *P. subcapitata* was calculated based on cell concentration between days 0 and 3, as previously described (Machado and Soares 2014).

Staining and microscopy analysis

The shape of the alga *P. subcapitata* was examined by microscopy image analysis. Randomly obtained photos of algal cells were acquired using a microscope equipped with phase-contrast lenses and a Leica DC 300F camera (Leica Microsystems, Heerbrugg, Switzerland). Photos were processed with Leica IM50-Image manager version 4.0 software (Leica Microsystems Imaging Solutions, Cambridge, UK). A minimum sample of 200 cells ($n \geq 200$) was used for each time and experiment.

The autofluorescence of the alga *P. subcapitata* was monitored by image analysis carried out by epifluorescence microscopy (EM). The microscope was equipped with an HBO-100 lamp and an I3 filter set, from Leica. Randomly and representative photos of algal cells were acquired using a N plan $\times 100$ objective and processed as described above. Overlaying of fluorescence and bright-field microscopy images was performed using ImageJ software (Schneider et al. 2012).

Cell death was assessed through the analysis of the integrity of the alga cell membrane using SYTOX Green (SG) dye, as previously described by Machado and Soares (2012). SG is a membrane-impermeant nucleic acid dye that stains algal cells which have lost their membrane integrity (SG

positive cells—dead cells) but does not penetrate in cells with the intact plasma membrane (SG negative cells—live cells) (Machado and Soares 2012). Algae were resuspended in OECD medium ($1 \times 10^6 \text{ mL}^{-1}$), incubated with $0.5 \mu\text{mol L}^{-1}$ of SG (Invitrogen, Eugene, OR, USA), in the dark, for 20 min, at 25°C , and observed by EM using a GFP filter set, from Leica. In each time and experiment, at least four samples of 100 cells ($n \geq 400$ cells) were counted in randomly selected microscope fields.

The analysis of the cell-division cycle progression of *P. subcapitata* was carried out by counting the number of nuclei. For this purpose, algal cells were stained with SYBR Green I (SGI). SGI was provided by Sigma-Aldrich (St. Louis, MO, USA). The probe (obtained from the supplier as $10,000\times$ concentrated) was diluted 10 times in dimethyl sulfoxide (DMSO, Sigma-Aldrich). Algal cells resuspended in OECD medium ($5 \times 10^6 \text{ mL}^{-1}$) were incubated with SGI $2.5\times$ concentrated (final concentration), in the dark, for 1 h, at 25°C , and observed by EM using a GFP filter set. Representative images (EM plus phase-contrast) were taken, in randomly selected microscope fields, using a N plan $\times 100$ objective, and processed as described above. A minimum sample of 400 cells ($n \geq 400$) was analyzed at each time and experiment.

Starch distribution in algae was analyzed after staining cells with Lugol dye. Lugol solution stains only starch, as it interacts with the spiral structure of the polysaccharide, giving a dark/black color; monosaccharides (glucose and fructose) do not react with Lugol (Gifuni et al. 2017). Cells were stained by combining 1.0 mL of algal suspension ($1 \times 10^6 \text{ mL}^{-1}$), in OECD medium, with $40 \mu\text{L}$ of 5% (w/v) Lugol solution; subsequently, the cell suspension was placed at 90°C , for 10 min. Digital images of stained algal cells were randomly obtained in a bright-field microscope, using a N plan $\times 100$ objective, and processed as described above.

The assessment of cellular lipid content was performed using BODIPY493/503 (Invitrogen, Carlsbad, CA, USA). For this purpose, algal cells resuspended in OECD medium ($5 \times 10^6 \text{ mL}^{-1}$) were incubated with $10 \mu\text{g mL}^{-1}$ BODIPY493/503 (final concentration), for 10 min, at 25°C . Then, cells were centrifuged ($2500\times g$, 5 min), washed three times with OECD medium, and resuspended in the same medium. Algal cells were observed using an EM equipped with the filter set GFP. Representative images were acquired using a N plan $\times 100$ objective and processed as described above; background subtraction was carried out using ImageJ software.

Pigment analysis

Photosynthetic pigments were extracted from algal cells ($3 \times 10^6 \text{ mL}^{-1}$) with 90% of acetone, for 20 h, at 4°C , as previously described by Soto et al. (2011). Then, cells were

centrifuged ($2500\times g$, 10 min), and the supernatant was recuperated and analyzed. The absorbance was measured at 630, 647, 664, and 691 nm for chlorophylls and at 480 nm for carotenoids. Absorbance was corrected (for turbidity) by subtracting the value of absorbance at 750 nm. Chlorophyll *a* (chl*a*) and *b* (chl*b*) content was determined as defined by Ritchie (2008). The content of carotenoids was calculated as described by Strickland and Parsons (1972). For each time and experiment, pigments content was determined in triplicate.

Photosynthetic performance

Photosynthetic activity was evaluated by pulse amplitude modulation (PAM) fluorometry using a junior PAM fluorometer (Walz, Effeltrich, Germany). Algal cells ($3 \times 10^6 \text{ mL}^{-1}$) were dark adapted for 30 min to maintain all photosystem II (PSII) reaction centers open; the minimal fluorescence (F_0) and the maximum fluorescence (F_m) yield were measured (tenfold), and the maximum photochemical quantum yield of PSII (F_v/F_m) (Maxwell and Johnson 2000) was automatically calculated using the WinControl software, version 3.2.2 (Walz 2000). Then, dark-adapted algal cells were illuminated by an actinic light (for closing all PSII centers) at an intensity of $190 \mu\text{mol m}^{-2} \text{ s}^{-1}$, and the minimum and the maximum fluorescence in the light (F'_0 and F'_m , respectively) were determined tenfold. These parameters were used to calculate the effective photochemical quantum yield of PSII (ΦPSII), the relative electron transport rate (ETR), and the non-photochemical quenching (NPQ) (Maxwell and Johnson 2000), using the WinControl software.

Reproducibility of the results and statistical analysis

All experiments were repeated, independently, at least three times. Results are presented as the mean \pm standard deviation (SD). Statistical differences among the results obtained regarding cell membrane integrity, photosynthetic pigments, and photosynthetic performance of algal cells were tested by one-way ANOVA followed by Tukey–Kramer multiple comparison method.

Results

Chronology of algae culture aging: cell number, death, and cell-division cycle

When incubated in OECD medium, the alga *P. subcapitata* grew exponentially during 3 days, with a duplication time of ~ 10.4 h, occurring a deceleration of growth on the 4th day. From the 5th day onwards, the number of cells ($\sim 5 \times 10^6 \text{ cells mL}^{-1}$) remained approximately constant (Fig. 1A).

The permanent loss of cell membrane integrity is one of the criteria used to define cell death (Galluzzi et al. 2018). Using the membrane-impermeant dye SG, it was possible to verify that until the 12th day of incubation, algae maintained an intact plasma membrane. With the aging of the culture, a small percentage of cells presented a compromised plasma membrane. At the end of the incubation period (21st day), ~7% of the cell population was dead (Fig. 1B).

The alga *P. subcapitata* reproduces asexually via auto-spores. Usually, during the cell-division cycle, *P. subcapitata* undergoes two nuclear divisions, originating four auto-spores which are released by the ruptured of the wall of the parental cell (Machado and Soares 2014; Van den Hoek et al. 1998). The analysis of the culture revealed the presence of cells with 1 to 4 nuclei during the exponential growth (first 3 days). For instance, on the 1st day after inoculation, 88.6%, 6.9%, and 4.5% of algal cells presented 1, 2, and 4 nuclei, respectively (Fig. 1C). The percentage of cells with one nucleus increases over time. Thus, on the 3rd day, the algal population was constituted of 95% of cells containing one nucleus. On the 5th day and subsequent days, almost all cell population ($\geq 99\%$) presents 1 nucleus (Fig. 1C). These results indicate that aged algal cells stopped dividing.

Together, the results described above allow the definition of three phases of *P. subcapitata* culture, their chronological sequence as well as the identification of three types of cells. Phase 1, between the inoculation day and the 4th day of incubation, corresponds to the proliferative phase (the period in which the number of algal cells increases as a result of cell division), being the culture constituted by a population of “young” cells. Phase 2, between the 5th and the 12th days, corresponds to the stationary phase, where cell division stops, but the cells keep their membrane intact (live cells). In this stage, cells begin to age. Phase 3, after the 12th day, corresponds to the death phase, where some cells lose their membrane integrity (dead cells); on the 21st day, the majority of the population (~93%) is composed of live, “old,” cells.

Aging-associated changes in algae

Cell shape modification

The microalga *P. subcapitata* exhibit, basically, two different shapes: lunate or helically twisted (Fig. 2; arrows 1 and 2, respectively) (Guiry and Guiry 2018; Machado and Soares 2020). The analysis of the algae morphology, over the incubation period, revealed that the lunate shape was predominant during the exponential growth, particularly during the first 2 days, where $\geq 97\%$ of “young” cells presented this form (Fig. 2). The percentage of cells with a lunate shape decline with the reach of the stationary phase. Between the 5th and 15th days, both shapes (lunate and helically twisted)

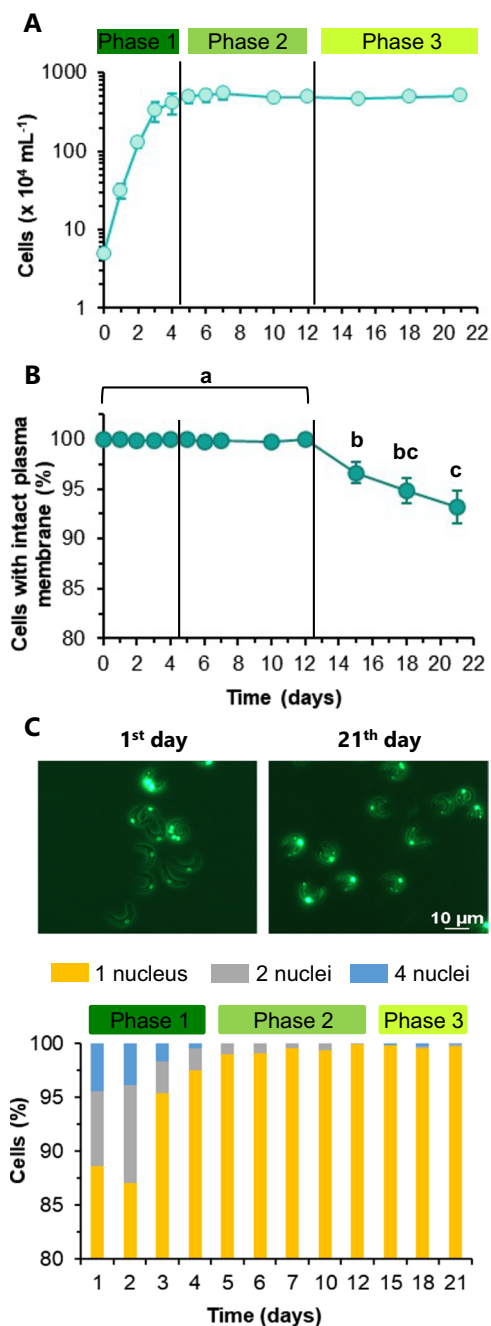


Fig. 1 Prolonged culture of *Pseudokirchneriella subcapitata* in OECD medium, in a batch mode. **A** Evolution of algal population. **B** Progression of cell membrane integrity; algae with compromised plasma membrane are considered dead. **C** Analysis of cell-division cycle progression (number of nuclei); representative microphotographs of the cells (observed by fluorescence plus phase-contrast microscopy) with different nuclei, at the beginning and end of incubation are shown. Phases of algal culture (marked by vertical dashed lines): 1—proliferative phase, period in which the number of cell increases as result of cell division; 2—stationary phase, where cells stop dividing but keep their membrane integrity; 3—death phase, which corresponds to the presence of cells with the compromised plasma membrane. For membrane integrity data, means with different letters are significantly different ($p < 0.05$, ANOVA; Tukey comparison test)

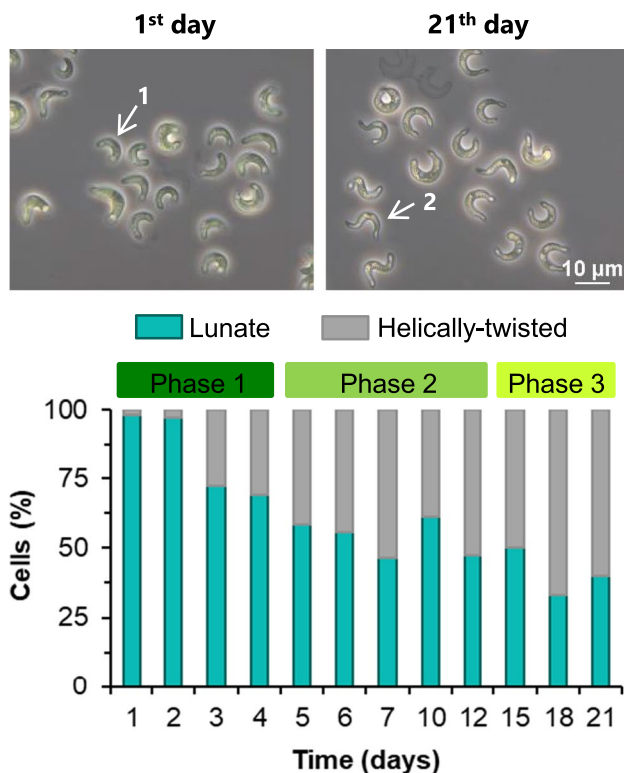


Fig. 2 Modification of the shape of the alga *P. subcapitata* during prolonged culture in OECD medium. Representative microphotographs of the algal culture at the beginning and end of incubation (1st and 21st days, respectively) are shown. Arrow 1: lunate shape. Arrow 2: helically twisted shape. Cells were observed by phase-contrast microscopy. Data are presented as mean values of at least three independent experiments. The culture phases (marked with bars of different colors) are defined in the legend of Fig. 1

co-exist in a proportion of approximately 50%. After the 15th day (during the death phase), aged cells presented, predominantly ($\geq 60\%$), a helically twisted shape (Fig. 2).

Concentration of photosynthetic pigments and photosynthetic activity

It was possible to observe a change in the appearance of the culture over time. The green color of the culture, presented in the proliferative phase (days 1 and 3), progressively decreased between the 5th and 10th days of incubation (stationary phase); later on, the continued aging of the culture resulted in its yellowish appearance (death phase) (Fig. 3A).

The change in the aspect of the culture with time (aging) could be correlated with the alteration of the algae photosynthetic pigments content. To validate this possibility, the cellular content of chl*a*, *b*, and carotenoids was quantified. As it can be seen in Fig. 3B, the cellular content of chl*a* was maintained, without significant alterations, until the 4th day of growth. On the 5th day of incubation, which corresponds to the beginning of the stationary phase, a sudden decay

(~65%) of this pigment was observed (Fig. 3B). A similar profile, although more drastic, was observed for chl*b*. In the first 3 days of growth, the levels of this pigment remained with small oscillations; however, on the 4th day, the concentration of chl*b* decreased by more than 90% (Fig. 3B). The quantification of carotenoids revealed a different profile when compared with chlorophylls. These pigments remained approximately constant until the 7th day of incubation. The diminution of carotenoids content was slower being only significantly different from the cells in the proliferative phase on the 10th day (Fig. 3B). During the death phase (after the 12th day), algal cells presented very low values of photosynthetic pigments (data not shown for chl*a* and *b*), which correspond to a decrease $> 98\%$ and 87% for chlorophylls and carotenoids, respectively.

Green algae exhibit intrinsic autofluorescence (AUF) due to the presence of photosynthetic pigments, being the main ones chl*a*, *b*, and carotenoids (Gantt 1975). AUF monitoring can be used to obtain information regarding the morphological and physiological state of cells (Monici 2005), namely, to assess the performance of the algal photosynthetic apparatus (Fai et al. 2007). During the proliferative phase (that is, until the 4th day), AUF had a similar intensity being distributed by all the cells, suggesting that chloroplast occupied a significant part of the algal cytosol (Fig. 4). At the beginning of the stationary phase (5th and 6th days), it was possible to observe an enhancement of orange AUF, not homogeneously distributed by the cell, which anticipates a reduction of the photochemistry efficiency. The light energy absorbed by photosynthetic pigments and not used to drive photosynthesis (photochemistry) can be dissipated as heat or re-emitted as AUF (Schiphorst and Bassi 2020). On the 7th and following days, despite orange-red AUF could be observed in part of the algae, there was a partial loss of AUF, mainly on algal tips, suggesting a shrinkage of the chloroplast. A drastic decay of AUF was observed on the 15th and following days (Fig. 4) (death phase), which is in agreement with the reduction of photosynthetic pigments described above.

A more detailed analysis of the impact of aging on photosynthesis was carried out by PAM fluorometry. “Young” algal cells, in the proliferative phase, presented a maximum photochemical quantum yield of PSII (F_v/F_m) in the range of 0.62, which corresponds to the optimal value (0.62–0.64) described for *P. subcapitata* (Drábková et al. 2007; Machado et al. 2015; Van der Grinten et al. 2010). Following the trend observed with chl*a*, a significant decay of F_v/F_m occurred on the onset of the stationary phase (5th day of incubation) (Fig. 5), indicating a decline in the functioning of the reaction centers of PSII. The decrease of F_v/F_m accentuated with the aging of algae, presenting a dropping of 32% and 68% (compared with day 0) after 5 and 10 days, respectively. In “old” cells, between 12 and 21 days of incubation, this parameter reached the minimum level (corresponded to a

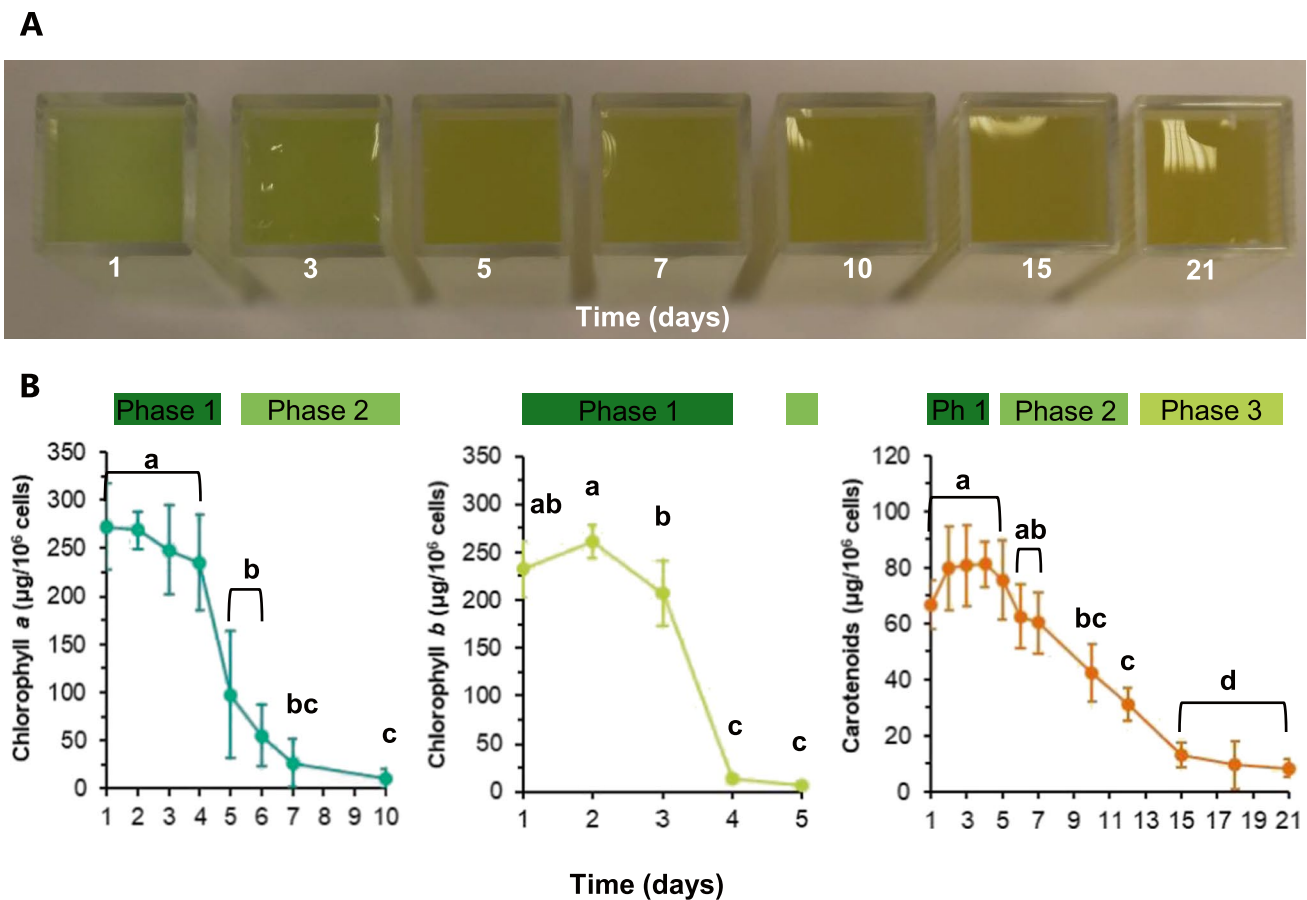


Fig. 3 Evolution of photosynthetic pigments content during long-term culturing of *P. subcapitata*. **A** Macroscopic visualization of the appearance of the culture over time. **B** Modification of chlorophyll *a*, chlorophyll *b*, and carotenoids content over time. Data are presented

as mean values of at least three independent experiments; mean values with different letters are significantly different ($p < 0.05$, ANOVA; Tukey comparison test). The culture phases (marked with bars of different colors) are defined in the legend of Fig. 1

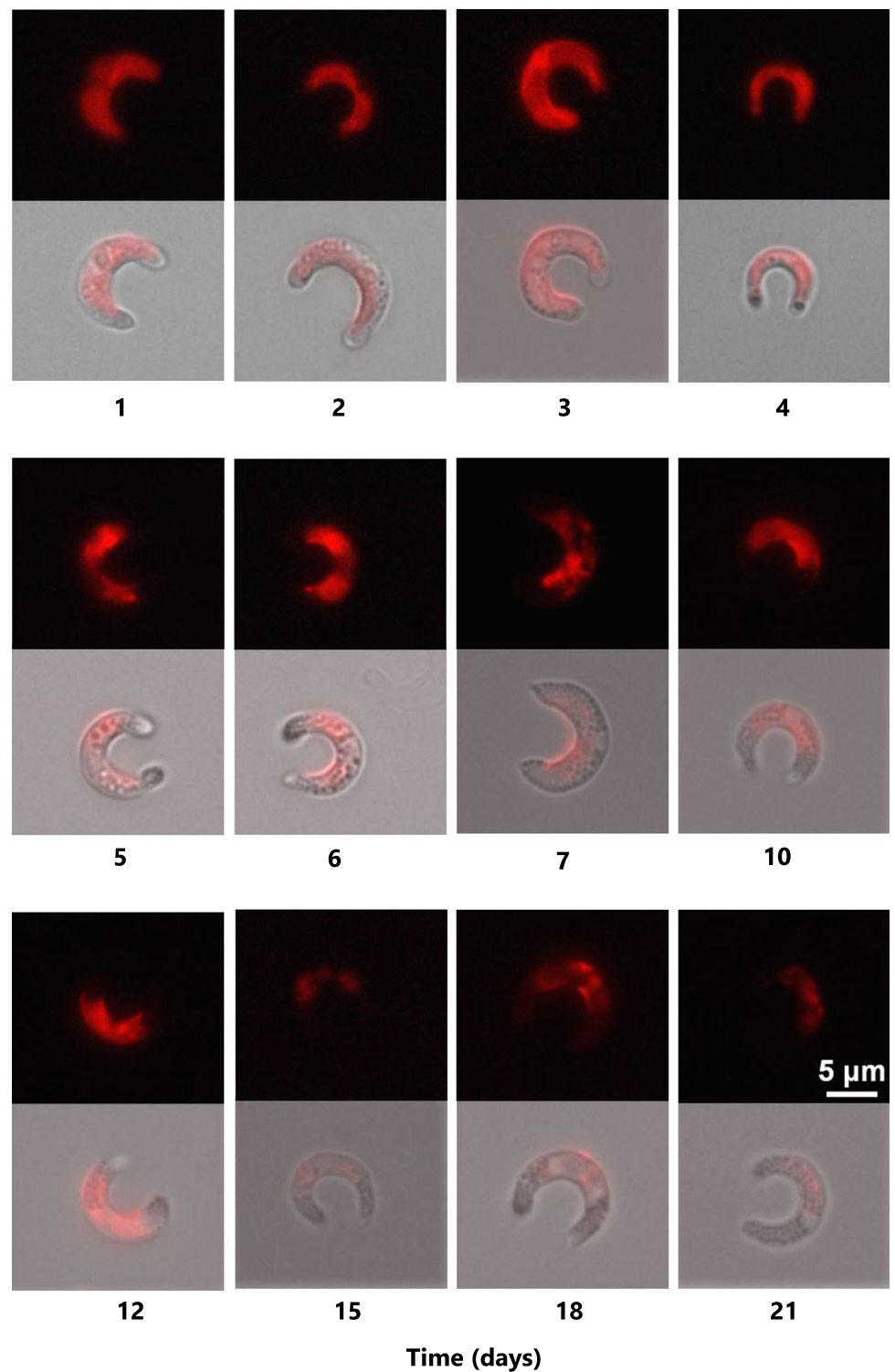
loss of ~81%, compared with “young” cells) (Fig. 5), suggesting that aging has a deep impact on the conversion efficiency of light energy of the PSII reaction centers. Up to the 6th day of incubation, no significant differences were observed in the effective photochemical quantum yield of PSII (ϕ_{PSII}) (Fig. 5). This parameter determines the portion of light adsorbed by chlorophyll, in PSII, that is used photochemically (Maxwell and Johnson 2000). On the 7th day, ϕ_{PSII} presented a decay of 55% (compared with day 0). From the 10th day, low values of ϕ_{PSII} were observed, which correspond to a diminution of 77% of this parameter (Fig. 5). The assessment of the flow rate of electrons through the photosynthetic chain, ETR (Consalvey et al. 2005), revealed a decline of 50% on the 7th day and ~75% from the 10th day (Fig. 5). Non-photochemical quenching (NPQ) is an adaptive mechanism displayed by PSII light-harvesting system, in plants and green algae, to cope with stress conditions (Horton and Ruban 2005; Müller et al. 2001). An increase of NPQ values was particularly observed at the beginning of the stationary phase (6th and 7th days), followed by a

progressive decrease, until reaching the values found in the exponential growth phase (Fig. 5), suggesting a transient induction of the mechanisms associated with the dissipation of excitation energy in excess of that which can be used to photochemistry. In resume, the results presented above, taken together, indicate that the aging of algae is associated with a decline in their photosynthetic activity and, probably, a shrinkage of the chloroplast.

Starch and neutral lipids content

Algal cells produce considerable amounts of lipids and carbohydrates being largely studied in order to be used for biodiesel production (Hossain et al. 2019; Schenk et al. 2008) and/or as a source of biopolymers (Aswathi Mohan et al. 2022; Madadi et al. 2021). However, it is unknown the profile of lipids and carbohydrates production by *P. subcapitata* over long-term culturing in OECD medium. So, the content of these compounds was evaluated by image microscopy analysis. During the proliferative phase (first 4 days), cells

Fig. 4 Follow-up of *P. subcapitata* autofluorescence over time. Representative microphotographs obtained by fluorescence and bright-field superimposed with fluorescence microscopy are shown

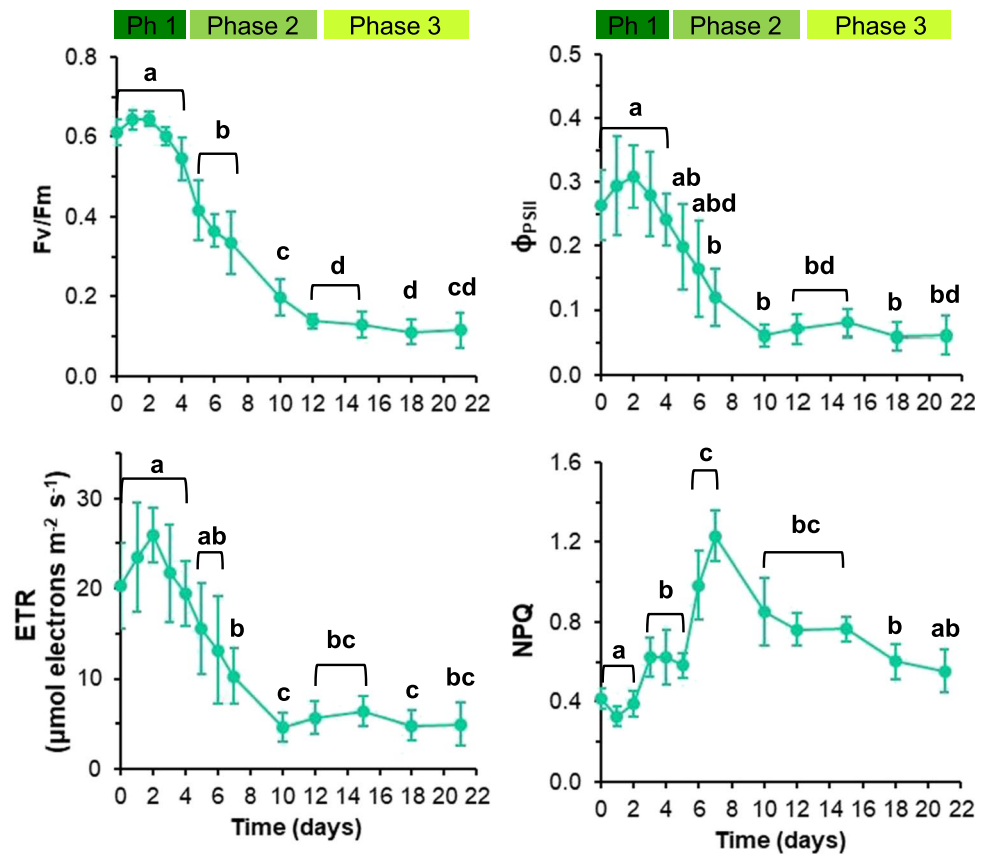


presented the highest starch content, observable by the brownish hue of the algal cytoplasm. Starch content progressively declined, over time, particularly after the 7th day (Fig. 6).

On the other hand, the neutral lipids, visualized using BODIPY 493/503 dye, were present in a few amounts in the

cytoplasm of algae, as fine globules, during the first 2 days (Fig. 6). Between the 3rd and 4th days, cellular lipid droplets increased in size and fluorescence, suggesting a strong intensification in its production; at this time, lipid droplets were mainly located at the ends of the cell. The number and size of lipid droplets increased sharply in the stationary phase

Fig. 5 Photosynthetic performance of *P. subcapitata* algal cells over prolonged culturing. Maximum photochemical quantum yield of PSII (F_v/F_m), effective photochemical quantum yield of PSII (Φ_{PSII}), relative electron transport rate (ETR), and non-photochemical quenching (NPQ) were assessed using PAM fluorescence assay. The data are presented as mean values from at least three independent experiments. Statistical differences were subjected to ANOVA followed by Tukey comparison test ($p < 0.05$) and are identified by different letters. The culture phases (marked with bars of different colors) are defined in the legend of Fig. 1



(after the 5th day), occupying the entire cytoplasm. In the last days of the assay (death phase), the green fluorescence became more diffuse, although the presence of lipid droplets throughout the cell continued to be detected (Fig. 6). These results show that in the alga *P. subcapitata*, the reserve compounds change remarkably between exponential growth, stationary, and death phases.

Discussion

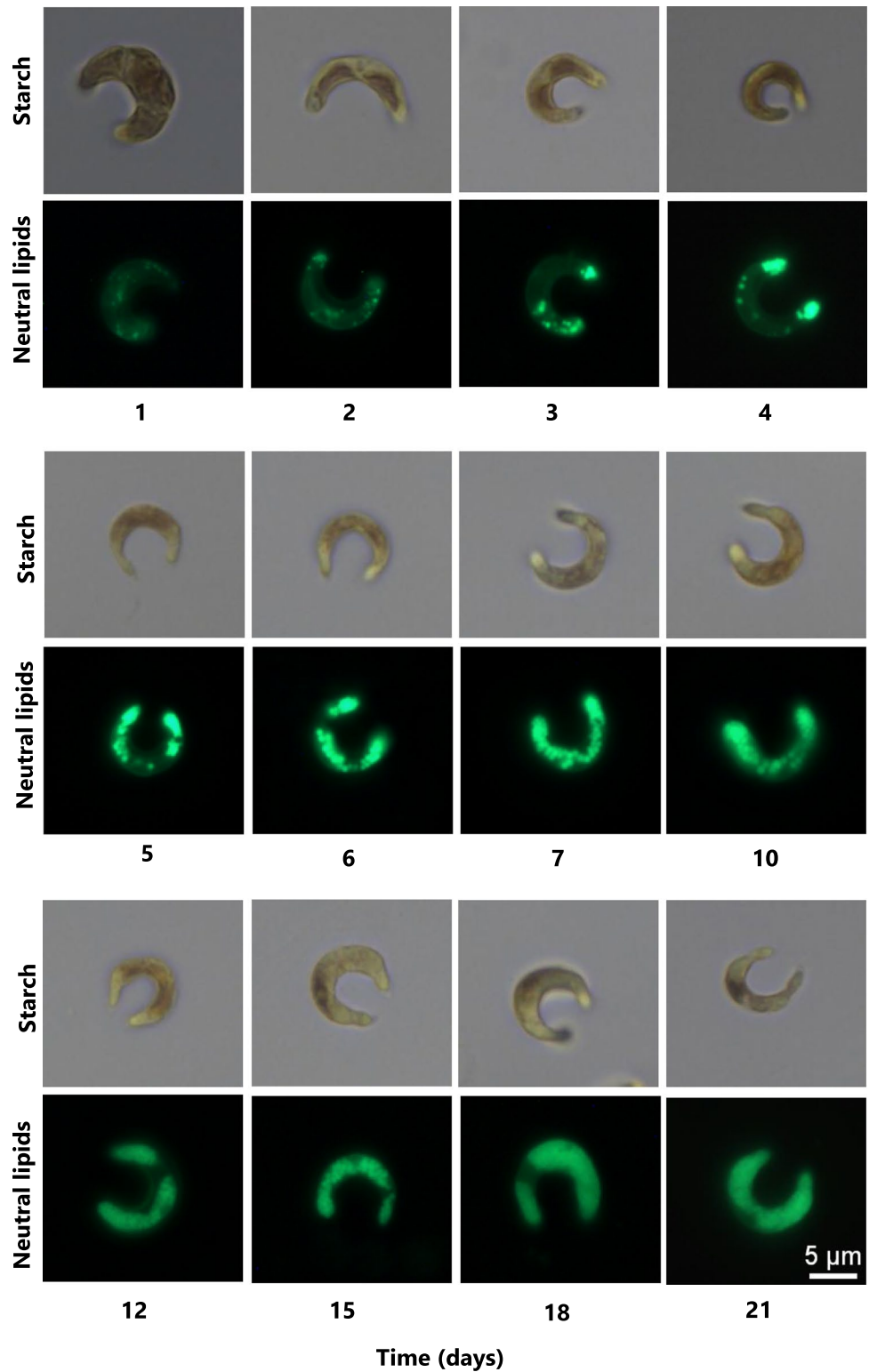
The microalga *P. subcapitata* constitutes a sensitive cellular model in the evaluation of ecotoxicity (OECD 2011; USEPA 2012), and it also has a considerable commercial interest, namely, as feedstock for aquaculture feed (Nagappan et al. 2021; Patil et al. 2007) or the production of biofuels (Benasla and Hausler 2020; Del Río et al. 2017). Whatever the use, the understanding and characterization of *P. subcapitata* physiology over long-term culturing, in the OECD medium, is of great importance and contributes to the characterization of the aging process of this alga.

After the *P. subcapitata* culture reached the stationary phase (5th day after inoculation), the number of cells remained approximately constant, and almost all population ($\geq 99\%$) presented one nucleus, which indicates the cessation of the cell-division cycle, a typical feature of

the chronological aging in microbial cells (Florea 2017). Although the number of cells remained constant during the incubation in the OECD medium, a small percentage of cells started to lose membrane integrity (dead cells) after the 12th day of incubation. However, throughout the incubation period, the majority of the population ($\sim 93\%$) was composed of live cells. The leakage of intracellular compounds from the dead cells may have occurred (due to the alteration of plasma membrane permeability), which allowed the supply of nutrients to the “old” cells, enabling their survival and increasing their longevity (extending their lifespan). In other words, cell death (as an altruistic suicide of presumably weakest cells) may be an adaptive strategy that makes possible to maximize the viability of the culture during its aging, as it was proposed for the yeast cells (Fröhlich and Madeo 2000). In the microalga *C. reinhardtii*, distinct behaviors were described depending if the algae are responding to an individual or combined nutrient deprivation. Considering individual stress (only one nutrient limitation), *C. reinhardtii* cultures maintained cell density for at least a month without significant death (Yang et al. 2018). The sum of several stresses led to a rapid decay of cell number shortly after the stationary phase (Humby et al. 2013; Kamalanathan et al. 2016).

During the stationary phase, a sharp reduction of chlorophylls content was observed, a similar effect to what takes

Fig. 6 Visualization of carbohydrates and neutral lipids in *P. subcapitata* over time. Photomicrographs of cells stained with Lugol (starch observation) or BODIPY 493/503 (lipids monitoring) and examined by bright-field or epifluorescence microscopy, respectively



place in senescing leaves where a shift in gene expression occurs, coinciding with a massive chlorophyll degradation (Andersson et al. 2004). It was suggested that in algal cells, chlorophylls can be degraded, under nitrogen limitations, for nutrient recycling (Msanne et al. 2012). Besides chlorophylls

reduction, a progressive decline of the maximum and effective photochemical quantum yield of PSII, F_v/F_m and Φ_{PSII} , respectively, were observed. These results are different from those described in the green alga *C. reinhardtii*, where the amount of chlorophyll and F_v/F_m remained constant through

the stationary phase (Damoo and Durnford 2021; Humby et al. 2013; Puzanskiy et al. 2018). This difference can be attributed to the higher sensitivity of *P. subcapitata* alga to stress. “Old” cells of *P. subcapitata* (after the 12th day of incubation) presented lower values of F_v/F_m and Φ_{PSII} , suggesting a big disturbance of photosynthesis. In a similar way, it was described that the decay of F_v/F_m and Φ_{PSII} in *C. reinhardtii* (Humby et al. 2013) and diatoms (*Phaeodactylum tricornutum* and *Chaetoceros muelleri*) (Liang et al. 2006) maintained for a prolonged period in the culture medium.

Chlorophylls play a central role in light harvesting (in antennae complexes) and transfer energy to the reaction centers (Schiphorst and Bassi 2020). Therefore, the decline of chlorophylls content, described above, can explain, at least partially, the decrease in photosynthetic efficiency (Φ_{PSII}). In addition, the decay of chlorophylls may have originated the deterioration of photosynthetic complexes, with the consequent diminution of the quantum efficiency (F_v/F_m); the reduction of F_v/F_m occurred in the stationary phase can also be associated with the damage of PSII, as a consequence of light stress. During this phase, the photosynthetic electron transport (ETR) in *P. subcapitata* was severely reduced, which implies that less energy is directed toward photosynthesis. As a short-term response to this stress, algal cells can activate reversible photo-protection mechanisms, such as NPQ or AUF, to redirect energy not used in photosynthesis (Horton and Ruban 2005). In fact, an increase in NPQ values and AUF were observed in the transition from exponential growth to the stationary phase and in the beginning of the stationary phase, indicating an energy dissipation.

It was also verified that up to the 7th day, carotenoid levels remained approximately constant. It is known that carotenoids serve two key roles in plants and algae: as accessory light-harvesting pigments, absorbing light energy for use in photosynthesis (broadening the spectral range over which light can support photosynthesis) and providing photoprotection of the photosynthetic system via ROS scavenging or by NPQ (enhancing energy dissipation as heat) (Armstrong and Hearst 1996; Demmig-Adams 1990; Hashimoto et al. 2016). On the other hand, the reduction of carotenoid content after the 7th day can be associated with the decrease in the protection of reaction centers by NPQ, observed after this day.

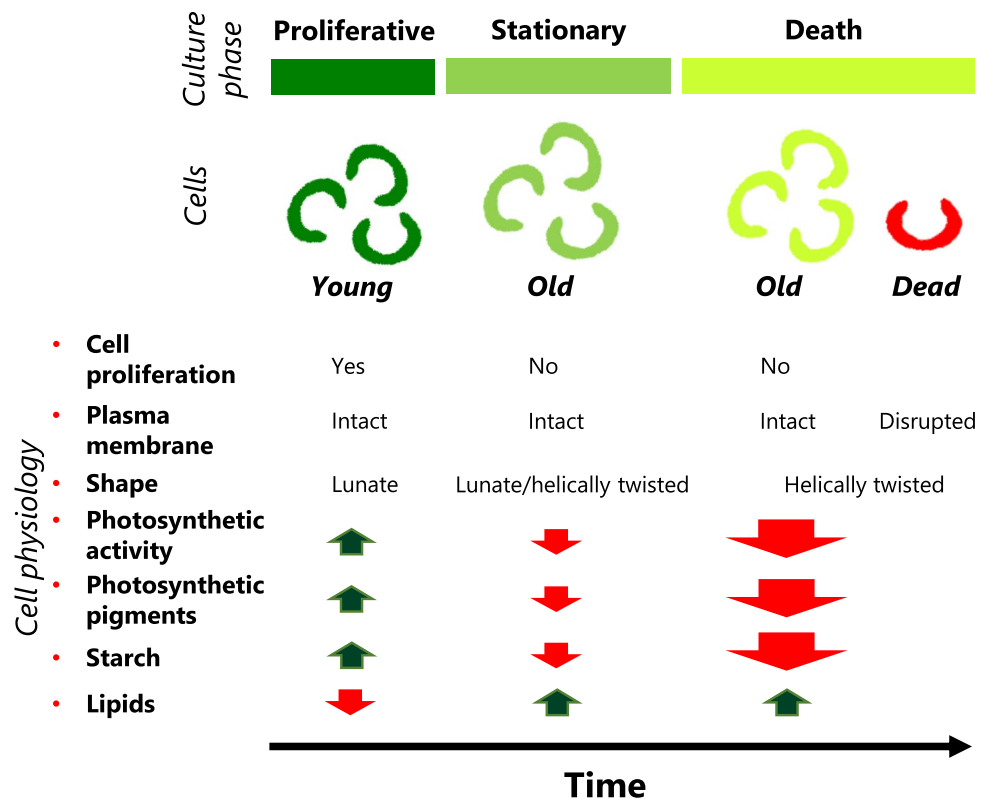
An increase of starch content in *P. subcapitata* algae growing exponentially (“young” cells) was observed; the content of this reserve compound decayed, gradually, in stationary and death phases (“old” cells). The increase of cellular starch content during the proliferative phase is supported by the maximum photosynthetic activity observed during this phase, which originates the carbon fixation and the carbohydrates storing, as starch, in microalgae. In agreement with this possibility, it was shown that the relative mRNA of

enzymes associated with photosynthesis, CO₂ fixation, and starch metabolism, in *Chorella* sp., was highly expressed during the exponential growth and reduced in the stationary phase (Cheng et al. 2017). Conversely, an intensification of lipid accumulation was observed in the transition from the proliferative phase to the stationary phase of *P. subcapitata* culture. Similar results were observed in *Chlamydomonas debaryana* (Sato and Toyoshima 2021) and in *Chorella* sp. (Cheng et al. 2017). Starch degradation and lipid content increase were also observed in different *Chorella* species (Brányiková et al. 2011; Li et al. 2015; Zhu et al. 2014), *Parachlorella kessleri* (Fernandes et al. 2013), *Scenedesmus obliquus* (Breuer et al. 2015), *C. reinhardtii*, and *Coccomyxa* sp. (Msanne et al. 2012), namely, in nitrogen-starved conditions. This stress condition affects growth and cell division, originating a change in algal metabolism and triacylglycerol accumulation (Merchant et al. 2012).

P. subcapitata also suffered changes in its shape, passing from a lunate form in the exponential growth to a predominantly helically twisted shape on the 18th day of incubation ($\geq 60\%$ of cells). This alga displays a rigid cell wall characterized by the presence of three layers (Fernández et al. 2021), being very hard to disrupt. It was reported that aging can cause severe changes in the cell walls of unicellular organisms (Florea 2017). In the case of the unicellular green algae *Spongiochloris typica*, the cell wall turned thinner in the stationary phase (McLean 1968). A similar effect may have occurred in *P. subcapitata*; the thinning of the cell wall may have allowed the alga to acquire another, not-so-rigid, shape.

To summarize, the incubation of *P. subcapitata* alga, in culture medium, for 21 days, with continuous agitation and light exposure, leads to a set of changes in the cells, being possible to observe three main phases in the culture and three categories of algal cells (“young” live, “old” live and dead cells) (Fig. 7). Phase one of the culture (proliferative phase) corresponds to the exponentially growing of “young” cells during the first 3 days, with a slowdown on the 4th day. The cultures present a typical green color. The population is practically 100% live, and the “young” cells display the maximum photosynthetic activity and photosynthetic pigments concentration. These “young” cells present, characteristically, a lunate morphology with the chloroplast occupying most of the cell and producing starch as reserve material. The second phase of the culture, between the 5th and the 12th days, corresponds to the stationary phase and the beginning of algae aging. After exponential growth, algae remain in a non-dividing stage ($\geq 99\%$ of cells with one nucleus), which can be a diagnostic feature of this phase. The aging of the cells has a consequence of an abrupt reduction of *chl a* and *b* content, responsible for reducing the green color of the culture. Chlorophylls breakdown can explain, at least partially, the decline of photosynthetic capacity (reduction of F_v/F_m

Fig. 7 Overview of the main phases of culture and the set of physiological changes associated with the aging of *P. subcapitata*, resulting from incubation of cells in OECD medium for 21 days, with continuous agitation and light exposure



and ϕ_{PSII}). The “old” cells present in this phase have a lower starch content and increased production of neutral lipids than “young” cells and, probably, present a shrinkage chloroplast. The death phase starts after the 12th day and is characterized by the presence of some cells with the compromised membrane (dead cells). However, almost all population (~93%) is composed of “old” live cells, which present a severe decline of photosynthetic activity (reduction > 75% of F_v/F_m and ϕ_{PSII}). At the end of the incubation period, between the 18th and 21st days, algal culture presents a yellowish color; “old” algal cells exhibit chloroplast AUF and starch content markedly reduced and, probably, lipid remetabolization begins.

This work contributes to the understanding and characterization of cytological and biochemical features associated with the stationary phase and chronological aging of *P. subcapitata*. This information can be useful from a fundamental and applied point of view, namely, in the application of this alga in toxicity studies or in obtaining biotechnological products.

Author contribution MM: validation, formal analysis, investigation, writing—original draft preparation, and visualization. ES: conceptualization, validation, writing—original draft preparation, review and editing, visualization, and supervision.

Funding This study was supported by the Portuguese Foundation for Science and Technology (FCT) under the scope of the strategic funding

of UIDB/04469/2020 unit. Manuela D. Machado thanks FCT for funding through program DL 57/2016-Norma Transitória.

Data availability All data generated or analyzed during this study are included in this published article.

Declarations

Ethics approval This article does not contain any studies with human participants or animals performed by any of the authors.

Consent for publication All authors have read and approved the final version of the manuscript for publication.

Conflict of interest The authors declare no competing interests.

References

Andersson A, Keskitalo J, Sjödin A, Bhalerao R, Sterky F, Wissel K, Tandre K, Aspeborg H, Moyle R, Ohmiya Y, Bhalerao R, Brunner A, Gustafsson P, Karlsson J, Lundeberg J, Nilsson O, Sandberg G, Strauss S, Sundberg B, Uhlen M, Jansson S, Nilsson P (2004) A transcriptional timetable of autumn senescence. *Genome Biol* 5:R24. <https://doi.org/10.1186/gb-2004-5-4-r24>

Armstrong GA, Hearst JE (1996) Genetics and molecular biology of carotenoid pigment biosynthesis. *FASEB J* 10:228–237. <https://doi.org/10.1096/fasebj.10.2.8641556>

Aswathi Mohan A, Robert Antony A, Greeshma K, Yun J-H, Ramanan R, Kim H-S (2022) Algal biopolymers as sustainable resources for a net-zero carbon bioeconomy. *Bioresour Technol* 344:126397. <https://doi.org/10.1016/j.biortech.2021.126397>

- Atikij T, Syaputri Y, Iwahashi H, Praneenararat T, Sirisattha S, Kagayama H, Waditee-Sirisattha R (2019) Enhanced lipid production and molecular dynamics under salinity stress in green microalga *Chlamydomonas reinhardtii* (137C). *Mar Drugs* 17:484. <https://doi.org/10.3390/md17080484>
- Benasla A, Hausler R (2020) Growth and production of lipids in *Raphidocelis subcapitata* immobilized in sodium alginate beads. *Energies* 13:506. <https://doi.org/10.3390/en13020506>
- Bondioli P, Della Bella L, Rivolta G, Chini Zittelli G, Bassi N, Rodolfi L, Casini D, Prussi M, Chiaramonti D, Tredici MR (2012) Oil production by the marine microalgae *Nannochloropsis* sp. F&M-M24 and *Tetraselmis suecica* F&M-M33. *Bioresour Technol* 114:567–572. <https://doi.org/10.1016/j.biortech.2012.02.123>
- Borowitzka MA (2013) High-value products from microalgae—their development and commercialisation. *J Appl Phycol* 25:743–756. <https://doi.org/10.1007/s10811-013-9983-9>
- Brányiková I, Maršálková B, Doucha J, Brányik T, Bišová K, Zachleder V, Vítová M (2011) Microalgae—novel highly efficient starch producers. *Biotechnol Bioeng* 108:766–776. <https://doi.org/10.1002/bit.23016>
- Breuer G, Martens DE, Draaisma RB, Wijffels RH, Lamers PP (2015) Photosynthetic efficiency and carbon partitioning in nitrogen-starved *Scenedesmus obliquus*. *Algal Res* 9:254–262. <https://doi.org/10.1016/j.algal.2015.03.012>
- Cheng D, Li D, Yuan Y, Zhou L, Li X, Wu T, Wang L, Zhao Q, Wei W, Sun Y (2017) Improving carbohydrate and starch accumulation in *Chlorella* sp. AE10 by a novel two-stage process with cell dilution. *Biotechnol Biofuels* 10:75. <https://doi.org/10.1186/s13068-017-0753-9>
- Cid A, Prado R, Rioboo C, Suarez-Bregua P, Herrero C (2013) Use of microalgae as biological indicators of pollution: looking for new relevant cytotoxicity endpoints. In: Johnsen MN (ed) *Microalgae: Biotechnology, microbiology and energy*. Nova Science Publishers Inc, New York, pp 311–324
- Consalvey M, Perkins RG, Paterson DM, Underwood GJC (2005) PAM fluorescence: a beginners guide for benthic diatomists. *Diatom Res* 20:1–22. <https://doi.org/10.1080/0269249X.2005.9705619>
- Damoo DY, Durnford DG (2021) Long-term survival of *Chlamydomonas reinhardtii* during conditional senescence. *Arch Microbiol* 203:5333–5344. <https://doi.org/10.1007/s00203-021-02508-y>
- Del Río E, García-Gómez E, Moreno JG, Guerrero M, García-González M (2017) Microalgae for oil. Assessment of fatty acid productivity in continuous culture by two high-yield strains, *Chlorococcum oleofaciens* and *Pseudokirchneriella subcapitata*. *Algal Res* 23:37–42. <https://doi.org/10.1016/j.algal.2017.01.003>
- Demmig-Adams B (1990) Carotenoids and photoprotection in plants: a role for the xanthophyll zeaxanthin. *Biochim Biophys Acta - Bioenerg* 1020:1–24. [https://doi.org/10.1016/0005-2728\(90\)90088-L](https://doi.org/10.1016/0005-2728(90)90088-L)
- Drábková M, Matthijs HCP, Admiraal W, Maršálek B (2007) Selective effects of H₂O₂ on cyanobacterial photosynthesis. *Photosynthetica* 45:363–369. <https://doi.org/10.1007/s11099-007-0062-9>
- Fai PB, Grant A, Reid B (2007) Chlorophyll a fluorescence as a biomarker for rapid toxicity assessment. *Env Toxicol Chem* 26:1520–1531. <https://doi.org/10.1897/06-394R1.1>
- Fernandes B, Teixeira J, Dragone G, Vicente AA, Kawano S, Bišová K, Přibyl P, Zachleder V, Vítová M (2013) Relationship between starch and lipid accumulation induced by nutrient depletion and replenishment in the microalga *Parachlorella kessleri*. *Bioresour Technol* 144:268–274. <https://doi.org/10.1016/j.biortech.2013.06.096>
- Fernández C, Asselborn V, Parodi ER (2021) Toxic effects of chlorpyrifos, cypermethrin and glyphosate on the non-target organism *Selenastrum capricornutum* (Chlorophyta). *An Acad Bras Cienc* 93:e20200233. <https://doi.org/10.1590/0001-3765202120200233>
- Florea M (2017) Aging and immortality in unicellular species. *Mech Ageing Dev* 167:5–15. <https://doi.org/10.1016/j.mad.2017.08.006>
- Fröhlich KU, Madeo F (2000) Apoptosis in yeast—a monocellular organism exhibits altruistic behaviour. *FEBS Lett* 473:6–9. [https://doi.org/10.1016/s0014-5793\(00\)01474-5](https://doi.org/10.1016/s0014-5793(00)01474-5)
- Galluzzi L, Vitale I, Aaronson SA, Abrams JM, Adam D, Agostinis P, Alnemri ES, Altucci L, Amelio I, Andrews DW, Annicchiarico-Petruzzelli M, Antonov AV, Arama E, Baehrecke EH, Barlev NA, Bazan NG, Bernassola F, Bertrand MJM, Bianchi K, Blagosklonny MV, Blomgren K, Borner C, Boya P, Brenner C, Campanella M, Candi E, Carmona-Gutierrez D, Cecconi F, Chan FK-M, Chandel NS, Cheng EH, Chipuk JE, Cidlowski JA, Ciechanover A, Cohen GM, Conrad M, Cubillos-Ruiz JR, Czabotar PE, D'Angiolella V, Dawson TM, Dawson VL, De Laurenzi V, De Maria R, Debatin K-M, DeBerardinis RJ, Deshmukh M, Di Daniele N, Di Virgilio F, Dixit VM, Dixon SJ, Duckett CS, Dynlacht BD, El-Deiry WS, Elrod JW, Fimia GM, Fulda S, García-Sáez AJ, Garg AD, Garrido C, Gavathiotis E, Golstein P, Gottlieb E, Green DR, Greene LA, Gronemeyer H, Gross A, Hajnoczky G, Hardwick JM, Harris IS, Hengartner MO, Hetz C, Ichijo H, Jäättelä M, Joseph B, Jost PJ, Juin PP, Kaiser WJ, Karin M, Kaufmann T, Kepp O, Kimchi A, Kitsis RN, Klionsky DJ, Knight RA, Kumar S, Lee SW, Lemasters JJ, Levine B, Linkermann A, Lipton SA, Lockshin RA, López-Otín C, Lowe SW, Luedde T, Lugli E, MacFarlane M, Madeo F, Malewicz M, Malorni W, Manic G, Marine J-C, Martin SJ, Martinou J-C, Medema JP, Mehlen P, Meier P, Melino S, Miao EA, Molkenin JD, Moll UM, Muñoz-Pinedo C, Nagata S, Nuñez G, Oberst A, Oren M, Overholtzer M, Pagano M, Panaretakis T, Pasparakis M, Penninger JM, Pereira DM, Pervaiz S, Peter ME, Piacentini M, Pinton P, Prehn JHM, Puthalakath H, Rabinovich GA, Rehm M, Rizzuto R, Rodrigues CMP, Rubinsztein DC, Rudel T, Ryan KM, Sayan E, Scorrano L, Shao F, Shi Y, Silke J, Simon H-U, Sistigu A, Stockwell BR, Strasser A, Szabadkai G, Tait SWG, Tang D, Tavernarakis N, Thorburn A, Tsujimoto Y, Turk B, Vanden Berghe T, Vandenabeele P, Vander Heiden MG, Villunger A, Virgin HW, Vousden KH, Vucic D, Wagner EF, Walczak H, Wallach D, Wang Y, Wells JA, Wood W, Yuan J, Zakeri Z, Zhivotovsky B, Zitvogel L, Melino G, Kroemer G (2018) Molecular mechanisms of cell death: recommendations of the Nomenclature Committee on Cell Death 2018. *Cell Death Differ* 25:486–541. <https://doi.org/10.1038/s41418-017-0012-4>
- Gantt E (1975) Phycobilisomes: light-harvesting pigment complexes. *Bioscience* 25:781–788. <https://doi.org/10.2307/1297221>
- Gao Y, Yang M, Wang C (2013) Nutrient deprivation enhances lipid content in marine microalgae. *Bioresour Technol* 147:484–491. <https://doi.org/10.1016/j.biortech.2013.08.066>
- Gershon H, Gershon D (2000) The budding yeast, *Saccharomyces cerevisiae*, as a model for aging research: a critical review. *Mech Ageing Dev* 120:1–22. [https://doi.org/10.1016/s0047-6374\(00\)00182-2](https://doi.org/10.1016/s0047-6374(00)00182-2)
- Gifuni I, Olivieri G, Pollio A, Franco TT, Marzocchella A (2017) Autotrophic starch production by *Chlamydomonas* species. *J Appl Phycol* 29:105–114. <https://doi.org/10.1007/s10811-016-0932-2>
- Guiry MD, Guiry GM (2018) *AlgaeBase*. World-wide electronic publication, National University of Ireland, Galway. <http://www.algaebase.org>; Accessed on 27 July 2022
- Hashimoto H, Uragami C, Cogdell RJ (2016) Carotenoids and photosynthesis. In: Stange C (ed) *Carotenoids in nature: biosynthesis, regulation and function*. Springer International Publishing, Cham, Switzerland, pp 111–139
- Horton P, Ruban A (2005) Molecular design of the photosystem II light-harvesting antenna: photosynthesis and photoprotection. *J Exp Bot* 56:365–373. <https://doi.org/10.1093/jxb/eri023>
- Hossain N, Mahlia TMI, Saidur R (2019) Latest development in microalgae-biofuel production with nano-additives. *Biotechnol Biofuels* 12:125. <https://doi.org/10.1186/s13068-019-1465-0>

- Humby PL, Snyder ECR, Durnford DG (2013) Conditional senescence in *Chlamydomonas reinhardtii* (Chlorophyceae). *J Phycol* 49:389–400. <https://doi.org/10.1111/jpy.12049>
- Kamalanathan M, Pierangelini M, Shearman LA, Gleadow R, Beardall J (2016) Impacts of nitrogen and phosphorus starvation on the physiology of *Chlamydomonas reinhardtii*. *J Appl Phycol* 28:1509–1520. <https://doi.org/10.1007/s10811-015-0726-y>
- Khan MI, Shin JH, Kim JD (2018) The promising future of microalgae: current status, challenges, and optimization of a sustainable and renewable industry for biofuels, feed, and other products. *Microb Cell Fact* 17:36. <https://doi.org/10.1186/s12934-018-0879-x>
- Koller M, Muhr A, Brauneegg G (2014) Microalgae as versatile cellular factories for valued products. *Algal Res* 6:52–63. <https://doi.org/10.1016/j.algal.2014.09.002>
- Li T, Gargouri M, Feng J, Park J-J, Gao D, Miao C, Dong T, Gang DR, Chen S (2015) Regulation of starch and lipid accumulation in a microalga *Chlorella sorokiniana*. *Bioresour Technol* 180:250–257. <https://doi.org/10.1016/j.biortech.2015.01.005>
- Liang Y, Beardall J, Heraud P (2006) Changes in growth, chlorophyll fluorescence and fatty acid composition with culture age in batch cultures of *Phaeodactylum tricornutum* and *Chaetoceros muelleri* (Bacillariophyceae). *Bot Mar* 49:165–173. <https://doi.org/10.1515/BOT.2006.021>
- Longo VD, Shadel GS, Kaeberlein M, Kennedy B (2012) Replicative and chronological aging in *Saccharomyces cerevisiae*. *Cell Metab* 16:18–31. <https://doi.org/10.1016/j.cmet.2012.06.002>
- Machado MD, Soares EV (2012) Development of a short-term assay based on the evaluation of the plasma membrane integrity of the alga *Pseudokirchneriella subcapitata*. *Appl Microbiol Biotechnol* 95:1035–1042. <https://doi.org/10.1007/s00253-012-4185-y>
- Machado MD, Soares EV (2014) Modification of cell volume and proliferative capacity of *Pseudokirchneriella subcapitata* cells exposed to metal stress. *Aquat Toxicol* 147:1–6. <https://doi.org/10.1016/j.aquatox.2013.11.017>
- Machado MD, Soares EV (2020) Reproductive cycle progression arrest and modification of cell morphology (shape and biovolume) in the alga *Pseudokirchneriella subcapitata* exposed to metolachlor. *Aquat Toxicol* 222:105449. <https://doi.org/10.1016/j.aquatox.2020.105449>
- Machado MD, Lopes AR, Soares EV (2015) Responses of the alga *Pseudokirchneriella subcapitata* to long-term exposure to metal stress. *J Hazard Mater* 296:82–92. <https://doi.org/10.1016/j.jhazmat.2015.04.022>
- Madadi R, Maljaee H, Serafim S (2021) Microalgae as contributors to produce biopolymers. *Mar Drugs* 19:466. <https://doi.org/10.3390/md19080466>
- Maxwell K, Johnson GN (2000) Chlorophyll fluorescence - a practical guide. *J Exp Bot* 51:659–668. <https://doi.org/10.1093/jexbot/51.345.659>
- McLean RJ (1968) Ultrastructure of *Spongiochloris typica* during senescence. *J Phycol* 4:277–283. <https://doi.org/10.1111/j.1529-8817.1968.tb04696.x>
- McLean RJ (1969) Rejuvenation of senescent cells of *Spongiochloris typica*. *J Phycol* 5:32–37. <https://doi.org/10.1111/j.1529-8817.1969.tb02572.x>
- Merchant SS, Kropat J, Liu B, Shaw J, Warakanont J (2012) TAG, You're it! *Chlamydomonas* as a reference organism for understanding algal triacylglycerol accumulation. *Curr Opin Biotechnol* 23:352–363. <https://doi.org/10.1016/j.copbio.2011.12.001>
- Monici M (2005) Cell and tissue autofluorescence research and diagnostic applications. *Biotechnol Annu Rev* 11:227–256. [https://doi.org/10.1016/S1387-2656\(05\)1007-2](https://doi.org/10.1016/S1387-2656(05)1007-2)
- Msanne J, Xu D, Konda AR, Casas-Mollano JA, Awada T, Cahoon EB, Cerutti H (2012) Metabolic and gene expression changes triggered by nitrogen deprivation in the photoautotrophically grown microalgae *Chlamydomonas reinhardtii* and *Coccomyxa* sp. C-169. *Phytochemistry* 75:50–59. <https://doi.org/10.1016/j.phytochem.2011.12.007>
- Müller P, Li X-P, Niyogi KK (2001) Non-photochemical quenching. A response to excess light energy. *Plant Physiol* 125:1558–1566. <https://doi.org/10.1104/pp.125.4.1558>
- Nagappan S, Das P, AbdulQuadir M, Thaher M, Khan S, Mahata C, Al-Jabri H, Vatland AK, Kumar G (2021) Potential of microalgae as a sustainable feed ingredient for aquaculture. *J Biotechnol* 341:1–20. <https://doi.org/10.1016/j.jbiotec.2021.09.003>
- Naselli-Flores L, Padisák J (2022) Ecosystem services provided by marine and freshwater phytoplankton. *Hydrobiologia* 28:1–16. <https://doi.org/10.1007/s10750-022-04795-y>
- Nyström T (2003) Conditional senescence in bacteria: death of the immortals. *Mol Microbiol* 48:17–23. <https://doi.org/10.1046/j.1365-2958.2003.03385.x>
- OECD (2011) Test No 201: Freshwater alga and cyanobacteria, growth inhibition test. Organization for Economic Cooperation and Development, Paris, France. <https://doi.org/10.1787/9789264069923-en>
- Patil V, Källqvist T, Olsen E, Vogt G, Gislerød HR (2007) Fatty acid composition of 12 microalgae for possible use in aquaculture feed. *Aquac Int* 15:1–9. <https://doi.org/10.1007/s10499-006-9060-3>
- Petralia RS, Mattson MP, Yao PJ (2014) Aging and longevity in the simplest animals and the quest for immortality. *Ageing Res Rev* 16:66–82. <https://doi.org/10.1016/j.arr.2014.05.003>
- Puzanskiy R, Tarakhovskaya E, Shavarda A, Shishova M (2018) Metabolomic and physiological changes of *Chlamydomonas reinhardtii* (Chlorophyceae, Chlorophyta) during batch culture development. *J Appl Phycol* 30:803–818. <https://doi.org/10.1007/s10811-017-1326-9>
- Ritchie RJ (2008) Universal chlorophyll equations for estimating chlorophylls *a*, *b*, *c*, and *d* and total chlorophylls in natural assemblages of photosynthetic organisms using acetone, methanol, or ethanol solvents. *Photosynthetica* 46:115–126. <https://doi.org/10.1007/s11099-008-0019-7>
- Sato N, Toyoshima M (2021) Dynamism of metabolic carbon flow of starch and lipids in *Chlamydomonas debaryana*. *Front Plant Sci* 12:646498. <https://doi.org/10.3389/fpls.2021.646498>
- Schenk PM, Thomas-Hall SR, Stephens E, Marx UC, Mussgnug JH, Posten C, Kruse O, Hankamer B (2008) Second generation biofuels: high-efficiency microalgae for biodiesel production. *Bio-Energy Res* 1:20–43. <https://doi.org/10.1007/s12155-008-9008-8>
- Schiphorst C, Bassi R (2020) Chlorophyll-xanthophyll antenna complexes: in between light harvesting and energy dissipation. In: Grossman AR, Raven JA (eds) *Larkum AWD*. Springer International Publishing, Switzerland, pp 27–55. https://doi.org/10.1007/978-3-030-33397-3_3
- Schneider CA, Rasband WS, Eliceiri KW (2012) NIH Image to ImageJ: 25 years of image analysis. *Nat Methods* 9:671–675. <https://doi.org/10.1038/nmeth.2089>
- Soto P, Gaete H, Eliana Hidalgo M (2011) Assessment of catalase activity, lipid peroxidation, chlorophyll-a, and growth rate in the freshwater green algae *Pseudokirchneriella subcapitata* exposed to copper and zinc. *Lat Am J Aquat Res* 39:280–285. <https://doi.org/10.3856/vol39-issue2-fulltext-9>
- Strickland J, Parsons TR (1972) A practical handbook of seawater analysis, 2nd edn. Fisheries Research Board of Canada, Ottawa
- Teh KY, Loh SH, Aziz A, Takahashi K, Effendy AWM, Cha TS (2021) Lipid accumulation patterns and role of different fatty acid types towards mitigating salinity fluctuations in *Chlorella vulgaris*. *Sci Rep* 11:438. <https://doi.org/10.1038/s41598-020-79950-3>
- US-EPA (2002) Methods for measuring the acute toxicity of effluents and receiving waters to freshwater and marine organisms. EPA-821-R-02-012. 5th edn. United States Environmental Protection Agency, Washington, DC, USA

- US-EPA (2012) Algal toxicity (OCSPP 850.4500). Ecological effects test guidelines. Office of Chemical Safety and Pollution Prevention. United States Environmental Protection Agency. EPA 712-C-006. Washington, DC, USA
- Van den Hoek C, Mann DG, Jahns HM (1998) Algae: an introduction to phycology. Cambridge University Press, Cambridge UK
- Van der Grinten E, Pikkemaat MG, van den Brandhof E-J, Stroomberg GJ, Kraak MHS (2010) Comparing the sensitivity of algal, cyanobacterial and bacterial bioassays to different groups of antibiotics. *Chemosphere* 80:1–6. <https://doi.org/10.1016/j.chemosphere.2010.04.011>
- Walz H (2000) WinControl window software for PAM fluorometers. In: Walz H (ed) Users manual. Heinz Walz GmbH, f Effeltrich Germany
- Yang L, Chen J, Qin S, Zeng M, Jiang Y, Hu L, Xiao P, Hao W, Hu Z, Lei A, Wang J (2018) Growth and lipid accumulation by different nutrients in the microalga *Chlamydomonas reinhardtii*. *Biotechnol Biofuels* 11:40. <https://doi.org/10.1186/s13068-018-1041-z>
- Zhu S, Huang W, Xu J, Wang Z, Xu J, Yuan Z (2014) Metabolic changes of starch and lipid triggered by nitrogen starvation in the microalga *Chlorella zofingiensis*. *Bioresour Technol* 152:292–298. <https://doi.org/10.1016/j.biortech.2013.10.092>

Publisher's note Springer Nature remains neutral with regard to jurisdictional claims in published maps and institutional affiliations.

Springer Nature or its licensor (e.g. a society or other partner) holds exclusive rights to this article under a publishing agreement with the author(s) or other rightsholder(s); author self-archiving of the accepted manuscript version of this article is solely governed by the terms of such publishing agreement and applicable law.